Journal of Peptide Science, Vol. 2, 106–116 (1996)

Effects of End Group and Aggregation on Helix Conformation: Crystal Structure of Ac-(Aib-Val-Ala-Leu)$_2$-Aib-OMe*

ISABELLA L. KARLE[1], JUDITH L. FLIPPEN-ANDERSON[1], KUCHIBHOTLA UMA[2] and PADMANABHAN BALARAM[2]

[1]Laboratory for the Structure of Matter, Naval Research Laboratory, Washington, DC, USA
[2]Molecular Biophysics Unit, Indian Institute of Science, Bangalore, India

Received 30 June 1995
Accepted 3 November 1995

The role of end groups in determining stereochemistry and packing in hydrophobic helical peptides has been investigated using an α-aminosobutyric acid (Aib) containing model nonapeptide sequence. In contrast to the Boc-analogue, Ac-(Aib-Val-Ala-Leu)$_2$-Aib-OMe crystallizes with two independent molecules in a triclinic cell. The cell parameters are: space group P1, $a = 10.100(2)$Å, $b = 15.194(4)$ Å, $c = 19.948(5)$ Å, $\alpha = 63.12(2)°$, $\beta = 88.03(2)°$, $\gamma = 88.61(2)°$, $Z = 2$, $R = 7.96\%$ for 5140 data where $|F_o| > 3\sigma(F)$. The two independent molecules alternate in infinite columns formed by head-to-tail hydrogen bonding. The helices in the two independent molecules are quite similar to each other but one molecule is rotated ~123° about its helix axis with respect to the other. All the helical columns pack parallel to each other in the crystal. Replacement of the bulky Boc group does not lead to any major changes in conformation. Packing characteristics are also similar to those observed for similar helical peptides.

Keywords: all parallel helix assemblies; helix transition; 3_{10}-/α-helices; two conformers; water associated with non-polar helices; X-ray crystallography

INTRODUCTION

The ready crystallizability of α-aminoisobutyric acid (Aib) containing peptides may be attributed to the ability of these residues to promote helical conformations [1–5] and the facility of cylindrical peptides to pack into ordered arrays in single crystals. A large number of accurate structural analyses of helical peptides ranging in length from 7 to 16 residues has permitted many insights into modes of association, hydration and conformational transition between 3_{10}- and α-helical structures in crystals [6–15]. In the large majority of these structures the peptides have been hydrophobic, neutral and contain protecting groups at the amino (frequently, *t*-butyloxycarbonyl, Boc) and carboxyl (most often, methyl esters, OMe) termini. Helical peptide aggregation in crystals has, almost without exception, been mediated by head-to-tail arrangement of molecules, with either direct peptide–peptide hydrogen bonds or water-mediated interactions of NH and CO groups, not involved in intramolecular hydrogen bonds [2,6]. It was therefore of interest to examine a structure in which the bulky *t*-butyloxycarbonyl (Boc) group is replaced by a small acetyl (Ac) group. This report describes the structure in crystals of a nonapeptide, Ac-Aib-Val-Ala-Leu-Aib-Val-Ala-Leu-Aib-OMe (**1**) and compares the results obtained with the structure of the corresponding Boc-protected peptide reported earlier [16].

Abbreviations: Aib, α-aminoisobutyric acid; Boc, *t*-butyloxycarbonyl

Address for correspondence: Dr Isabella L. Karle, Laboratory for the Structure of Matter, Naval Research Laboratory, Washington, DC 20375-5341, USA. Fax: 202-767-6874

Supplementary material consisting of bond lengths, bond angles, anisotropic thermal parameters and coordinates for H atoms are available from the Cambridge Crystallographic Data Centre. Observed and calculated structure factors can be obtained from ILK. For ordering instructions see Notes for Contributors.31

CCC 1075-2617/96/020106-11

Experimental procedures

Peptide Synthesis

Peptide **1** was synthesized by conventional solution phase procedures [17] and purified by reverse-phase HPLC on a C_{18} column (10 μm) using methanol–water gradients. All intermediates were checked for purity by HPLC (C_{18}) and 270 MHz ^{1}H-NMR spectra (data not shown).

Boc-Val-Ala-Leu-Aib-OMe (2). 10.85 g (50 mmol) of Boc-Val-OH in 50 ml DMF were cooled to 0°C. 13.5 g (45 mmol) of H-Ala-Leu-Aib-OMe [17] was added, followed by 12.36 g (~60 mmol) of *N, N'*-dicyclohexylcarbodiimide (DCC) and 6.7 g (50 mmol) of 1-hydroxybenzotriazole (HOBT). After stirring for 40 h, the reaction mixture was diluted with EtOAc (150 ml) and *N, N'*-dicyclohexylurea (DCU) filtered off. The filtrate was washed with brine (50 ml), 2N HCl (3 × 50 ml), 1M Na_2CO_3 and evaporation *in vacuo*, a solid was obtained. Yield, 21 g (84%).

Boc-Val-Ala-Leu-Aib-OH (3). 7.0 g (14 mmol) of **2** were dissolved in MeOH (15 ml) and 2N NaOH (15 ml). The reaction mixture was stirred at room temperature and the progress of reaction was followed by TLC. On completion of the reaction, methanol was evaporated, water added and the aqueous layer washed with ether. It was then acidified with 2N HCl and extracted with EtOAc (3 × 40 ml). The combined organic layer was passed through Na_2SO_4 and was evaporated, to yield a white solid. Yield, 6.8 g (100%).

H-Val-Ala-Leu-Aib-OMe (4). 14.0 g (28 mmol) of 2 were deprotected using 98% formic acid (30 ml). The reaction was followed by TLC. On completion of reaction, formic acid was evaporated, the residue dissolved in water (50 ml) and washed with ether (2 × 30 ml). The aqueous layer was neutralized with Na_2CO_3 and extracted with EtOAc (3 × 80 ml). The organic layer was dried over Na_2SO_4 and evaporated *in vacuo* to yield a gum, which was ninhydrin positive. Yield, 10.75 g (96%).

Boc-Aib-Val-Ala-Leu-Aib-OMe (5). 2.0 g (10 mmol) of Boc-Aib-OH were coupled to 4.0 g (10 mmol) of 4 in 10 ml DMF using 2.4 g (11.6 mmol) of DCC and 1.3 g (10 mmol) of HOBT, as described in the case of 2. Yield, 4.95 g (85%).

Boc-Aib-Val-Ala-Leu-Aib-OH (6). 4.5 g (7.7 mmol) of 5 were saponified using 8 ml of MeOH and 8 ml of 2N NaOH, as described in the case of **3**. Yield, 4.1 g (93%).

Boc-Aib-(Val-Ala-Leu-Aib)$_2$-OMe (7). 0.74 g (1.3 mmol) of 6 was coupled to a 0.48 g (1.2 mmol) of 4 in 3 ml DMF using 0.3 g (1.5 mmol) of DCC and 0.17 g (1.3 mmol) of HOBT, as described in the case of **2**. Yield, 0.85 g (69%). The crude peptide was purified on a silica gel column using 2.5% MeOH in $CHCl_3$ for elution. A fraction of this purified peptide was further purified by HPLC on an RP-18 column using a linear MeOH/H_2O gradient (75–85% MeOH in 20 min). Melting point, 205–206°C.

Ac-Aib-(Val-Ala-Leu-Aib)$_2$-OMe (1). 50 mg (0.05 mmol) of 7 were deprotected using 98% formic acid (0.5 ml) as described in the case of 4. The resulting free base was dissolved in a 1:1 mixture of acetic acid and acetic anhydride (1.5 ml). Progress of the reaction was followed by TLC. After completion of the reaction, the reaction mixture was diluted with water (2 ml) and evaporated to dryness. The residue was taken into EtOAc and washed with 1N HCl, 1M Na_2CO_3 and water. The organic layer was dried and evaporated to yield a solid. The crude product was purified by HPLC using a linear MeOH/H_2O gradient (70–95% MeOH in 25 min). The 270 MHz ^{1}H-NMR spectrum confirmed peptide identity. Melting point 232–234°C.

X-ray Crystallography

Crystals were grown from a CH_3OH/H_2O solution by slow evaporation. A dried crystal in the form of a prism, 0.20 × 0.25 × 0.45 mm, was used to collect X-ray diffraction data on an automated four-circle diffractometer using CuK_α radiation ($\lambda = 1.54178$ Å) and a graphice monochromator. The $\theta - 2\theta$ scan technique was used with a scan of $2.0° + 2\theta(\alpha_1) - 2\theta(\alpha_2)$, a variable scan rate of 7°/min to 14°/min, depending upon the diffracted intensity, and $2\theta_{max} = 112°$ (resolution 0.93 Å) for a total of 7115 unique reflections and 5140 reflections with intensities greater than $3\sigma(F)$. Three reflections, monitored after every 97 measurements, remained constant to within 2%. The cell parameters for space group P1 are $a = 10.100(2)$ Å, $b = 15.194(4)$ Å, $c = 19.948(5)$ Å, $\alpha = 63.12(2)°$, $\beta = 88.03(2)°$, $\gamma = 88.61(2)°$, $V = 2728.7$ Å^3, $Z = 2$. The calculated density for **2** ($C_{43}H_{77}N_9O_{12}$)·$4H_2O$ is 1.154 g/cm^3.

Table 1 Atomic Coordinates (x10^4) and Equivalent Isotropic Displacement Coefficients (Å^2 × 10^3)

	x	*y*	*z*	*U*(eq)[a]
C(1)	− 4475(18)	4922(14)	9598(9)	110(11)
O(0)	− 5165(10)	5141(7)	10016(5)	120(6)
C(2)	− 4668(16)	3987(11)	9504(10)	152(12)
N(1)	− 3522(11)	5530(9)	9155(6)	86(6)
C(1A)	− 3189(14)	6445(12)	9200(8)	98(9)
C(1′)	− 4416(12)	7084(9)	9154(7)	77(7)
O(1)	− 4558(8)	7539(7)	9515(5)	101(6)
C(1B1)	− 2471(13)	6205(14)	9925(9)	169(16)
C(1B2)	− 2270(12)	7032(11)	8509(9)	125(11)
N(2)	− 5304(10)	7163(7)	8627(5)	66(5)
C(2A)	− 6465(11)	7780(8)	8517(6)	63(6)
C(2′)	− 7377(13)	7488(10)	9201(7)	76(7)
O(2)	− 7976(8)	8077(6)	9351(5)	85(5)
C(2B)	− 7179(12)	7886(9)	7809(7)	74(7)
C(21G)	− 6325(12)	8452(10)	7101(7)	98(8)
C(22G)	− 8558(12)	8340(9)	7751(7)	99(8)
N(3)	− 7511(9)	6473(8)	9618(6)	71(6)
C(3A)	− 8353(12)	6140(9)	10276(7)	76(7)
C(3′)	− 7775(16)	6407(8)	10875(7)	77(7)
O(3)	− 8527(8)	6650(6)	11261(5)	88(5)
C(3B)	− 8602(14)	5058(10)	10602(7)	110(9)
N(4)	− 6439(11)	6355(8)	10942(6)	90(7)
C(4A)	− 5898(13)	6645(12)	11482(8)	95(9)
C(4′)	− 5994(12)	7729(13)	11192(10)	86(10)
O(4)	− 6211(8)	8029(7)	11680(5)	103(6)
C(4B)	− 4437(14)	6356(14)	11547(7)	139(13)
†C(4G)	− 3610(19)	6142(20)	12245(9)	175(31)
†C(41D)	− 4338(27)	5471(35)	12980(8)	212(32)
†C(42D)	− 2207(17)	5782(33)	12177(15)	168(26)
†C(4G′)	− 4348(33)	5249(14)	12119(15)	142(36)
†C(43D)	− 2914(42)	4878(29)	12265(24)	215(43)
†C(44D)	− 5176(64)	5005(36)	12838(21)	345(44)
N(5)	− 5856(10)	8345(10)	10467(7)	90(7)
C(5A)	− 6061(14)	9420(11)	10161(8)	88(8)
C(5′)	− 7433(12)	9646(9)	10445(6)	73(7)
O(5)	− 7511(8)	10205(6)	10720(5)	104(6)
C(51B)	− 6085(15)	9837(10)	9324(8)	125(10)
C(52B)	− 4928(14)	9853(13)	10406(9)	168(14)
N(6)	− 8451(11)	9172(7)	10369(5)	80(5)
C(6A)	− 9812(14)	9400(11)	10556(7)	99(8)
C(6′)	− 9940(13)	8948(11)	11422(8)	80(9)
O(6)	− 10608(9)	9401(7)	11701(5)	100(5)
C(6B)	− 10908(18)	9174(18)	10210(7)	182(16)
C(61G)	− 10793(18)	9656(17)	9362(7)	208(15)
†C(62G)	− 12102(33)	8607(37)	10658(16)	154(30)
†C(63G)	− 11187(43)	8083(17)	10563(21)	117(24)
N(7)	− 9363(9)	8091(8)	11846(5)	67(5)
C(7A)	− 9496(11)	7624(8)	12667(7)	65(6)
C(7′)	− 8796(11)	8208(8)	13008(7)	59(6)
O(7)	− 9228(7)	8155(6)	13621(5)	81(5)
C(7B)	− 8966(12)	6565(8)	12993(6)	84(7)
N(8)	− 7714(9)	8711(7)	12642(5)	68(5)

Continued...

Table 1 Continued

	x	*y*	*z*	*U*(eq)[a]
C(8A)	− 6985(11)	9273(9)	12938(6)	75(7)
C(8′)	− 7359(11)	10349(9)	12629(9)	65(7)
O(8)	− 7361(8)	10714(6)	13070(4)	85(4)
C(8B)	− 5457(12)	9233(10)	12722(7)	90(8)
C(8G)	− 4725(15)	8270(11)	13167(8)	99(9)
C(81D)	− 4547(14)	8107(10)	13978(8)	117(9)
C(82D)	− 3398(13)	8248(11)	12785(9)	131(11)
N(9)	− 7572(11)	10851(9)	11905(6)	88(6)
C(9A)	− 7811(15)	11912(9)	11559(7)	81(8)
C(9′)	− 6792(23)	12401(13)	11791(9)	118(11)
C(91B)	− 7631(14)	12274(9)	10709(7)	102(8)
C(92B)	− 9184(14)	12155(10)	11760(8)	115(10)
O(9)	− 6972(12)	13072(8)	11966(6)	134(7)
O(10)	− 5549(13)	12085(8)	11747(6)	124(7)
C(10)	− 4503(20)	12656(15)	11859(10)	204(16)
C(11)	− 432(12)	134(11)	3969(8)	77(8)
O(00)	− 660(8)	820(6)	4163(5)	85(5)
C(12)	− 1012(12)	216(10)	3275(7)	102(9)
N(11)	326(10)	− 636(7)	4353(6)	69(5)
C(11A)	739(12)	− 925(8)	5138(7)	68(6)
C(11′)	1447(11)	− 64(8)	5153(6)	58(6)
O(11)	1237(7)	157(5)	5676(4)	72(4)
C(11B)	− 459(14)	− 1241(9)	5659(7)	103(8)
C(11C)	1677(13)	− 1759(8)	5323(7)	103(8)
N(12)	2390(9)	370(6)	4641(5)	59(5)
C(12A)	3237(11)	1128(8)	4672(6)	62(6)
C(12′)	2502(11)	2090(9)	4461(7)	61(6)
O(12)	2641(7)	2552(6)	4833(4)	75(4)
C(12B)	4529(12)	1280(10)	4177(7)	85(8)
C(12G)	5294(12)	2165(11)	4104(7)	113(10)
C(12C)	5325(13)	317(11)	4461(9)	131(12)
N(13)	1699(10)	2392(7)	3886(5)	69(5)
C(13A)	912(13)	3300(9)	3676(7)	81(7)
C(13′)	− 9(14)	3196(9)	4305(8)	77(7)
O(13)	− 205(8)	3895(6)	4447(4)	85(4)
C(13B)	202(16)	3555(11)	2980(8)	139(11)
N(14)	− 588(8)	2333(8)	4709(6)	65(5)
C(14A)	− 1466(11)	2145(8)	5372(7)	68(6)
C(14′)	− 728(12)	2354(8)	5942(6)	61(6)
O(14)	− 1189(7)	2864(5)	6208(4)	69(4)
C(14B)	− 1943(10)	1080(9)	5725(7)	79(7)
C(14G)	− 2753(13)	773(11)	6473(8)	98(9)
C(14D)	− 4144(16)	1285(13)	6354(9)	159(13)
C(14E)	− 2814(15)	− 387(12)	6890(9)	163(12)
N(15)	409(9)	1821(6)	6192(5)	56(5)
C(15A)	1165(10)	1874(8)	6790(6)	55(6)
C(15′)	1422(10)	2962(8)	6582(7)	53(6)
O(15)	1247(7)	3295(5)	7029(4)	78(4)
C(15B)	2480(10)	1353(7)	6828(6)	69(6)
C(15C)	409(11)	1364(8)	7550(6)	79(6)
N(16)	1923(8)	3482(6)	5880(5)	56(4)
C(16A)	2385(12)	4485(8)	5669(6)	66(6)

Continued...

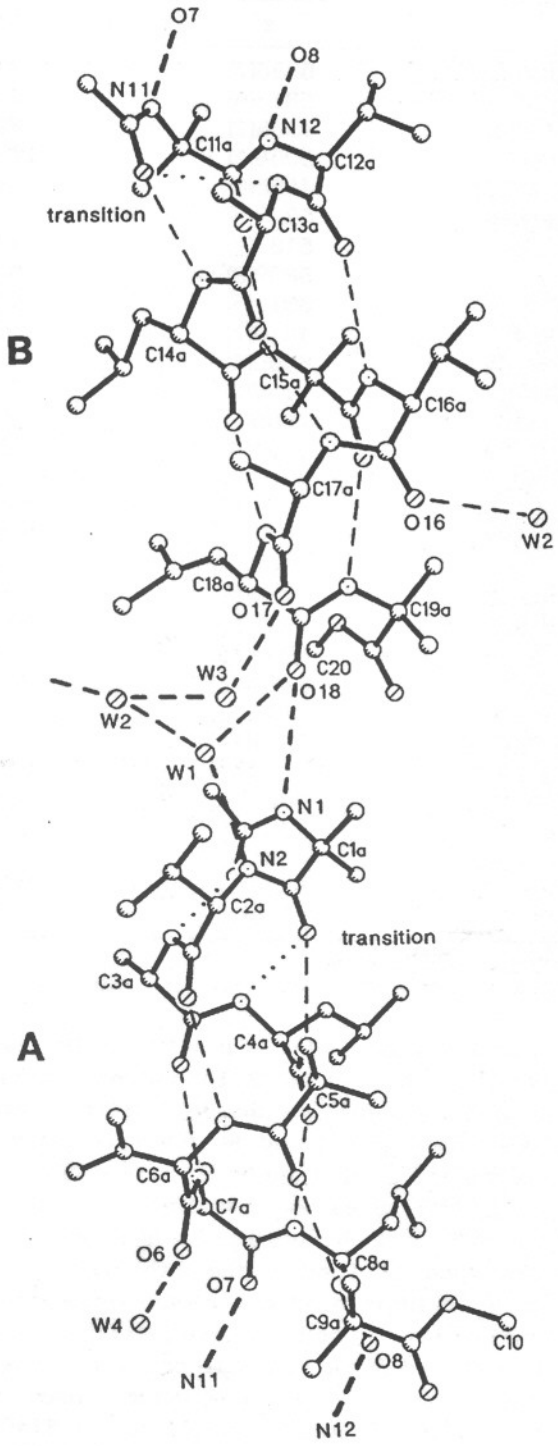

Figure 1 Helical conformation and hydrogen bonds in conformers A and B. Dashed lines represent intramolecular $5 \rightarrow 1$ NH···O hydrogen bonds, dotted lines represent $4 \rightarrow 1$ hydrogen bonds in or near the transition region between $4 \rightarrow 1$ and $5 \rightarrow 1$ bonds (3_{10}-helix to α-helix). Head-to-tail NH···O bonds, as well as peptide–water hydrogen bonds, are shown by heavy dashed lines.

RESULTS

The helices

The conformations of molecules A and B are shown in Figure 1. Continuous columns are formed by the alternation of molecules A and B connected by head-to-tail hydrogen bonding. The molecules are turned ~123°, with respect to each other, about the helix axis. Molecules A and B are very similar, but not identical. The backbone in A begins as a 3_{10}-helix with a N(3)···O(0) hydrogen bond, and goes through a transition between N(4) and N(5) to five α-helix hydrogen bonds; Figure 1 and Table 2. The backbone in B has six α-helix hydrogen bonds beginning with N(14)···O(00). The N(13) atom is within 3.268 Å of O(00); however, the N(13)H···O(00) distance is 2.83 Å, very long for an additional hydrogen bond to O(00) of a 3_{10}-type. The backbone in the Boc-analogue [16] has four α-helix hydrogen bonds, flanked by a 3_{10}-hydrogen bond at the N-terminal and the C-terminal.

A comparison of the ϕ,ψ angles for the three molecules of the same peptide is displayed graphi-

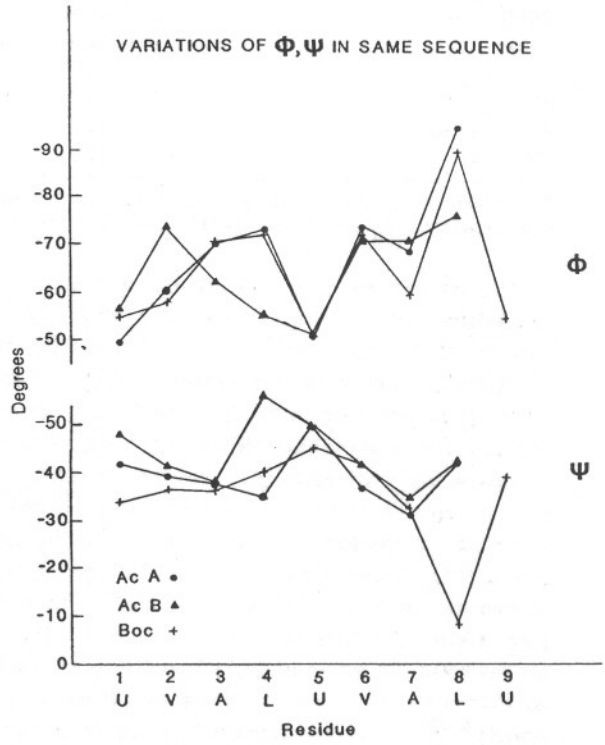

Figure 2 Comparison of torsional angles [21] ϕ(N–C$^{\alpha}$) and ψ(C$^{\alpha}$–C′) in the Ac- and Boc-analogues. The three molecules are represented by Ac–A ●, Ac–B ▲ and Boc- +. For both Ac conformers, there is a helix reversal at Aib[9]; since ϕ and ψ have positive values, they are not shown on this diagram.

Table 1 Continued

	x	*y*	*z*	*U*(eq)
C(16′)	1273(14)	5180(8)	5583(7)	71(6)
O(16)	1348(9)	5811(6)	5813(5)	99(5)
C(16B)	3227(13)	4827(8)	4935(7)	79(7)
C(16G)	4510(13)	4187(12)	5088(9)	128(11)
C(16E)	3604(15)	5900(10)	4655(8)	139(10)
N(17)	181(10)	5116(6)	5239(5)	71(5)
C(17A)	− 935(12)	5778(9)	5137(7)	71(6)
C(17′)	− 1679(13)	5583(13)	5869(9)	93(10)
O(17)	− 2163(10)	6299(7)	5916(5)	124(6)
C(17B)	− 1879(12)	5654(9)	4610(7)	103(8)
N(18)	− 1755(9)	4661(7)	6395(6)	68(5)
C(18A)	− 2505(11)	4427(9)	7108(7)	78(8)
C(18′)	− 1716(14)	4730(9)	7589(7)	77(7)
O(18)	− 2319(8)	5038(6)	7994(5)	100(6)
C(18B)	− 2739(12)	3310(9)	7496(8)	93(8)
C(18G)	− 3761(22)	2936(13)	7750(18)	298(23)
C(18D)	− 3724(25)	1825(20)	8168(20)	302(26)
C(18E)	− 5194(16)	3338(17)	7599(15)	223(21)
N(19)	− 404(11)	4520(8)	7634(6)	97(7)
C(19A)	470(17)	4668(15)	8135(11)	131(14)
C(19′)	− 289(21)	4136(25)	8956(15)	167(23)
O(19)	− 239(13)	4554(17)	9332(11)	285(21)
C(19B)	1761(13)	4191(16)	8132(11)	201(20)
C(19C)	606(18)	5691(20)	7864(14)	248(29)
O(20)	− 678(18)	3269(17)	9119(11)	205(16)
C(20)	− 1302(23)	2634(29)	9895(13)	342(32)
W1	− 5017(10)	6042(8)	7702(6)	139(7)
W2	3740(13)	6120(10)	6456(7)	192(90)
W3	− 4255(15)	7383(16)	5928(11)	291(17)
W4	− 12324(22)	10987(12)	11133(15)	372(20)

[a]Equivalent isotropic *U* defined as one-third of the trace of the orthogonalized U_{ij} tensor.
†Occupancy: 0.55 for C(4G), C(41D), C(42D); 0.45 for C (4G′), C(43D), C(44D); 0.47 for C(62G); 0.53 for C (63G).

The structure was solved by a vector-search procedure [18] and partial structure expansion [19] contained in the PATSEE program which is an independent program compatible with the SHELX84 package of programs [20]. The model for the vector search consisted of 28 backbone atoms from the Boc-analogue with the same peptide sequence [16]. Full-matrix least-squares refinement with anisotropic thermal parameters was performed on the coordinates of C, N and O atoms, except for the disordered atoms in side chains of Leu[4] and Val[6] of molecule A (see atoms marked with † in Table 1). Hydrogen atoms were placed in idealized positions and allowed to ride with the C or N atoms to which they were bonded. The thermal parameters for H atoms were not refined. They were arbitrarily chosen to be roughly proportional to the U_{eq} values of the C or N atoms to which they are bonded. Hydrogen atoms were omitted for the water molecules and two disordered side chains in molecule A. No disorder was found in molecule B. The approximate atomic positions for the disorder in Leu[4] and Val[6] in molecule A were found in difference maps. The occupancy of the alternate conformations was estimated from least-square refinement to be nearly 0.5 : 0.5 for each disorder. Some bond restraints were applied to bond lengths of the disordered side chains for the refinement. The least-squares program used for refining the 132 atom (C, N and O) structure is contained in the SHELXTL package of programs [18]. The weighting scheme used was $w^{-1} = \sigma^2(F) + 0.0002\ F^2$. The *R* factor for 5140 data (greater than $3\sigma(F)$ is 7.96% and $wR = 7.90\%$. The parameter to data ratio is 8.5 : 1.

Fractional coordinates of C, N and O atoms are listed in Table 1 with the atoms in partially occupied sites designated by †. Equivalent atoms in B are related to A by adding 10.

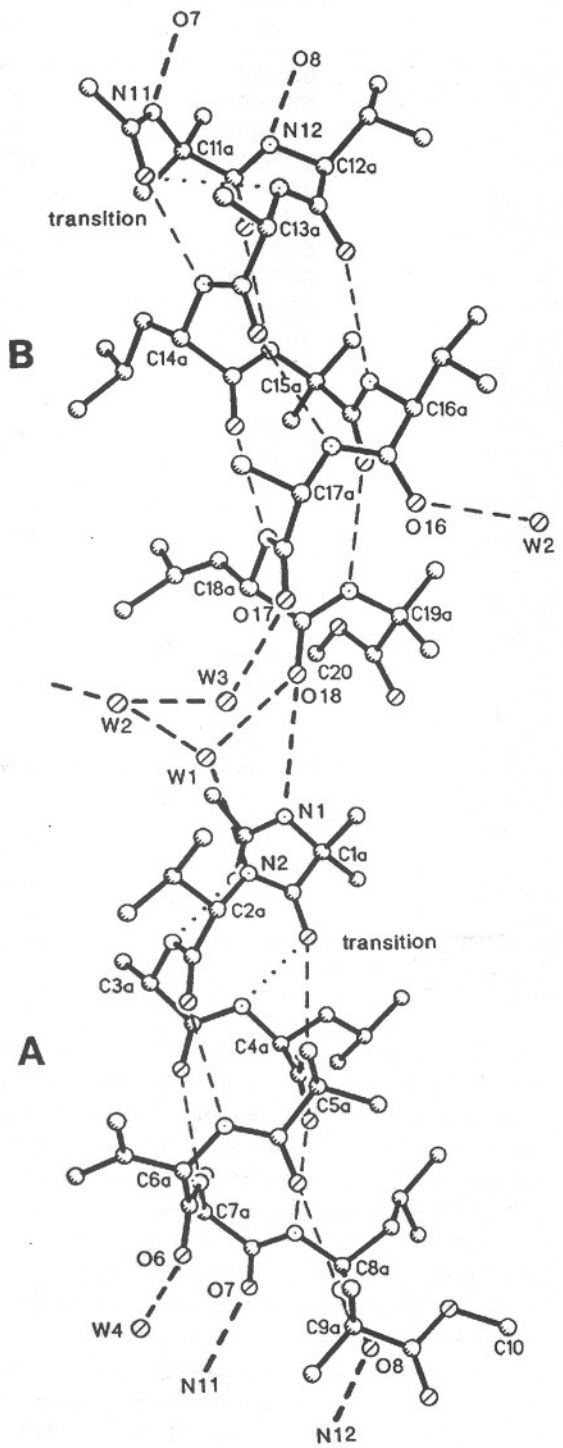

Figure 1 Helical conformation and hydrogen bonds in conformers A and B. Dashed lines represent intramolecular $5 \rightarrow 1$ NH···O hydrogen bonds, dotted lines represent $4 \rightarrow 1$ hydrogen bonds in or near the transition region between $4 \rightarrow 1$ and $5 \rightarrow 1$ bonds (3_{10}-helix to α-helix). Head-to-tail NH···O bonds, as well as peptide–water hydrogen bonds, are shown by heavy dashed lines.

RESULTS

The helices

The conformations of molecules A and B are shown in Figure 1. Continuous columns are formed by the alternation of molecules A and B connected by head-to-tail hydrogen bonding. The molecules are turned ~123°, with respect to each other, about the helix axis. Molecules A and B are very similar, but not identical. The backbone in A begins as a 3_{10}-helix with a N(3)···O(0) hydrogen bond, and goes through a transition between N(4) and N(5) to five α-helix hydrogen bonds; Figure 1 and Table 2. The backbone in B has six α-helix hydrogen bonds beginning with N(14)···O(00). The N(13) atom is within 3.268 Å of O(00); however, the N(13)H···O(00) distance is 2.83 Å, very long for an additional hydrogen bond to O(00) of a 3_{10}-type. The backbone in the Boc-analogue [16] has four α-helix hydrogen bonds, flanked by a 3_{10}-hydrogen bond at the N-terminal and the C-terminal.

A comparison of the ϕ,ψ angles for the three molecules of the same peptide is displayed graphi-

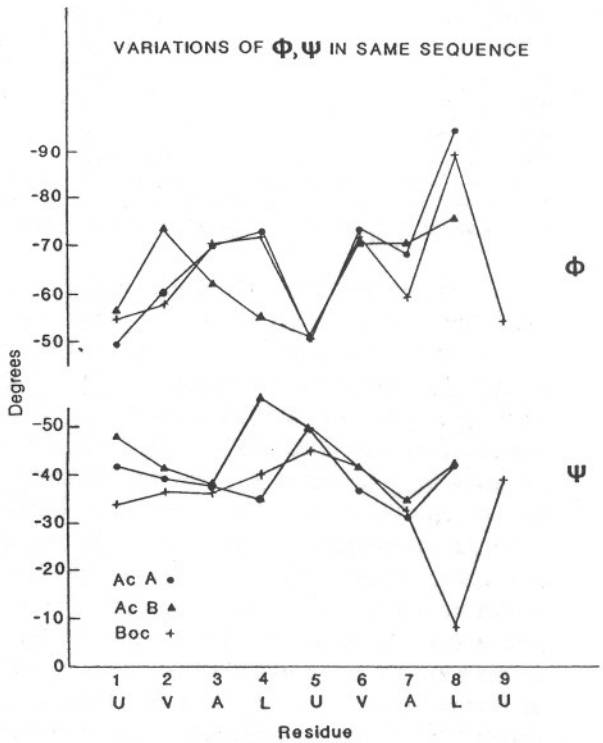

Figure 2 Comparison of torsional angles [21] ϕ(N–C$^{\alpha}$) and ψ(C$^{\alpha}$–C′) in the Ac- and Boc-analogues. The three molecules are represented by Ac–A ●, Ac–B ▲ and Boc- +. For both Ac conformers, there is a helix reversal at Aib[9]; since ϕ and ψ have positive values, they are not shown on this diagram.

Table 2 Hydrogen bonds[a]

Type	Donor	Acceptor	N—O,Å O—O	H–O,Å	angle° C=O···N
Head-to-tail	N1	O18	2.954	2.00	171
Peptide–solvent	N2	W1	3.028	2.07	
4 → 1	N3	O0	2.963	2.30	127
Transition	N4	O1	3.179	2.68[b]	110[b]
5 → 1	N5	O1	2.947	2.02	159
	N6	02	3.173	2.27	151
	N7	03	3.002	2.12	150
	N8	O4	2.929	2.09	159
	N9	O5	2.939	2.00	158
Solvent–peptide	W4	O6	2.750		
Head-to-tail	N11	O7[c]	2.837	1.90	140
	N12	O8[c]	2.937	2.12	147
4 → 1 Transition	N13	O00	3.268	2.83[b]	118
4 → 1	N14	O00	2.958	2.02	168
	N15	O11	3.218	2.28	148
	N16	O12	3.066	2.13	159
	N17	O13	2.969	2.04	156
	N18	O14	2.958	2.05	159
	N19	015	3.071	2.15	151
Solvent–peptide	W2	O16	2.918		
	W3	O17	2.654		
	W1	O18	3.033		
Solvent–solvent	W1	W2[d]	2.776		
	W2	W3[e]	2.666		

[a]The H atoms were placed in idealized positions with N–H = 0.96 Å.
[b]Poor geometry for 4 → 1 H bond.
[c]Symmetry equivalent $1+x, -1+y, -1+z$.
[d]Symmetry equivalent $-1+x$, y, z.
[e]Symmetry equivalent $1+x$, y, z.

cally in Figure 2 and Table 3. Although there are differences in these values for each residue, there is an overall agreement of the profiles except in two instances: Leu[4] for molecule B (labelled Leu[14]) and the last residue at the C-terminal. The reason for the deviation of the ϕ and ψ values of Leu[4] for molecule B from the profiles of the other two molecules is not immediately apparent except, perhaps, in the other two molecules there is a helix transition from 3_{10}- to α- at Leu[4] but there is no transition of this type in molecule B. The other major difference is at the C-terminal where there is helix reversal in both molecules of the Ac-analogue but a continuation of the right-handed helix in the Boc-analogue.

Side chains in the three molecules are either ordered or disordered (mainly into two distinct conformations) in the three molecules. A variety of conformations are assumed for the Val and Leu residues, probably dictated by the 'best' fit to the space available in the packing of the molecules in the crystals.

Head-to-tail Hydrogen Bonding.

The head-to-tail hydrogen bonding is different between A to B and B to A in the continuous helical column formed by the alternating molecules A and B, as well as in the Boc-crystal. In the direction A to B, Figure 1, there is one direct peptide hydrogen bond, N(1)···O(18) and the water-mediated hydrogen bond N(2)···W(1)···O(18). There is also a lateral network of hydrogen bonds O(17)– – –W(3)– – –W(2)– – –O(16). In the

W(1)– – –N(2)

direction B to A there are two different peptide

Table 3 Torsional Angles[a]

			Molecule A	Molecule B	Boc[b]
Ac	0	ω_0	+178	−167	
Aib	1	ϕ	−51	−57	−56
		ψ	−42	−49	−34
		ω	−177	−172	−178
Val	2	ϕ	−60	−73	−58
		ψ	−39	−41	−37
		ω	180	+177	−180
Ala	3	ϕ	−65	−62	−65
		ψ	−37	−38	−37
		ω	+178	+177	+178
Leu	4	ϕ	−73	−56	−72
		ψ	−34	−58	−40
		ω	+175	−175	+177
Aib	5	ϕ	−51	−51	−50
		ψ	−49	−50	−45
		ω	−175	−171	−179
Val	6	ϕ	−73	−71	−72
		ψ	−37	−41	−42
		ω	−178	−180	−180
Ala	7	ϕ	−67	−70	−59
		ψ	−31	−34	−33
		ω	−179	−178	−177
Leu	8	ϕ	−94	−75	−89
		ψ	−41	−42	−8
		ω	−174	−173	−171
Aib	9	ϕ	+49	+50	−54
		ψ	+49	+49	−39 (+139)[c]
		ω	+171	+175	+178 (−174)[c]
Side chains					
Val	2	$\chi_2^{1,1}$	−66	+171	−72
		$\chi_2^{1,2}$	+168	−60	+78
Leu	4	$\chi_4^{1,1}$	−55 (−83)[d]	+174	−80 (+179)[e]
		$\chi_4^{2,1}$	+46 (−177)[d]	+70	−180 (−167)[e]
		$\chi_4^{2,2}$	+175 (−78)[d]	−164	−68 (+68)[e]
Val	6	$\chi_6^{1,1}$	−56	−66	−61
		$\chi_6^{1,2}$	+131[d]	+174	+174
			+75[d]		
Leu	8	$\chi_8^{1,1}$	−75	−132	−63
		$\chi_8^{2,1}$	−70	+21	−61
		$\chi_8^{2,2}$	+166	−175	+174

[a]ESDs~1.0° for Ac analogue, ~1.2° for Boc analogue.
[b]Boc analogue [16].
[c]Alternate conformations of backbone at C-terminus of Boc analogue.
[d]Alternate conformations in disordered side chains in Ac analogue.
[e]Alternate conformations of disordered Leu[4] side chain in Boc analogue.

hydrogen bonds, N(11)···O(7) and N(12)···O(8). In this area there also is the hydrogen bond W(4)···O(6). The water molecule W(4) does not participate in any other hydrogen bonding.

In the Boc-analogue [16], where the molecules are stacked directly over each other only by translation (and no rotation as in the A···B···A stack), there is one direct head to tail hydrogen bond, N(1)—O(7), and a lateral network of solvent-mediated hydrogen bonds N(2)–W-(1)—W(2)—O(8) (or W(2) replaced by MeOH). The head-to-tail hydrogen bond network in the Boc-analogue has some similarities to the A to B hydrogen bond network described above for the Ac-analogue.

Parallel Aggregation of Peptide Molecules

If there were only one molecule in a triclinic cell, then completely parallel packing of helices would be mandatory. With more than one molecule per unit cell in a P1 crystal, packing of helices can be parallel, antiparallel or skewed. The present crystal provides still another example of all parallel packing of α-helices. Figure 3 shows the packing of the columns of helices. The individual molecules labelled A and B show a checkerboard arrangement. Molecules A···B···A in adjacent helical columns, in the direction along the short diagonal of the cell as shown in Figure 3, are rotated by about 123° with respect to each other. In the *a* direction, adjacent molecules in the helical columns are A···A···A or B···B···B and are repeated by one call edge translation. Most C···C interhelical approaches are 3.8–4.1 Å, except for a few, such as C81D···C16E ($-1+x$, y, $1+z$) (3.55 Å), C14D···C15B ($-1+x$, y, z) (3.52 Å) and C18E···C19B ($-1+x$, y, z) (3.62 Å).

CONCLUSIONS

The replacement of Ac- for Boc- as an end group has produced only minor variations in helix conformation and intramolecular hydrogen bonding, particularly since the number of NH and CO moieties has not changed. There have been some changes in the conformation of side chains of Leu and Val; however, such differences also occur between conformers in the same crystal and are not specifically related to the change of the end group. A new feature that has been found in this structure is the alternation of

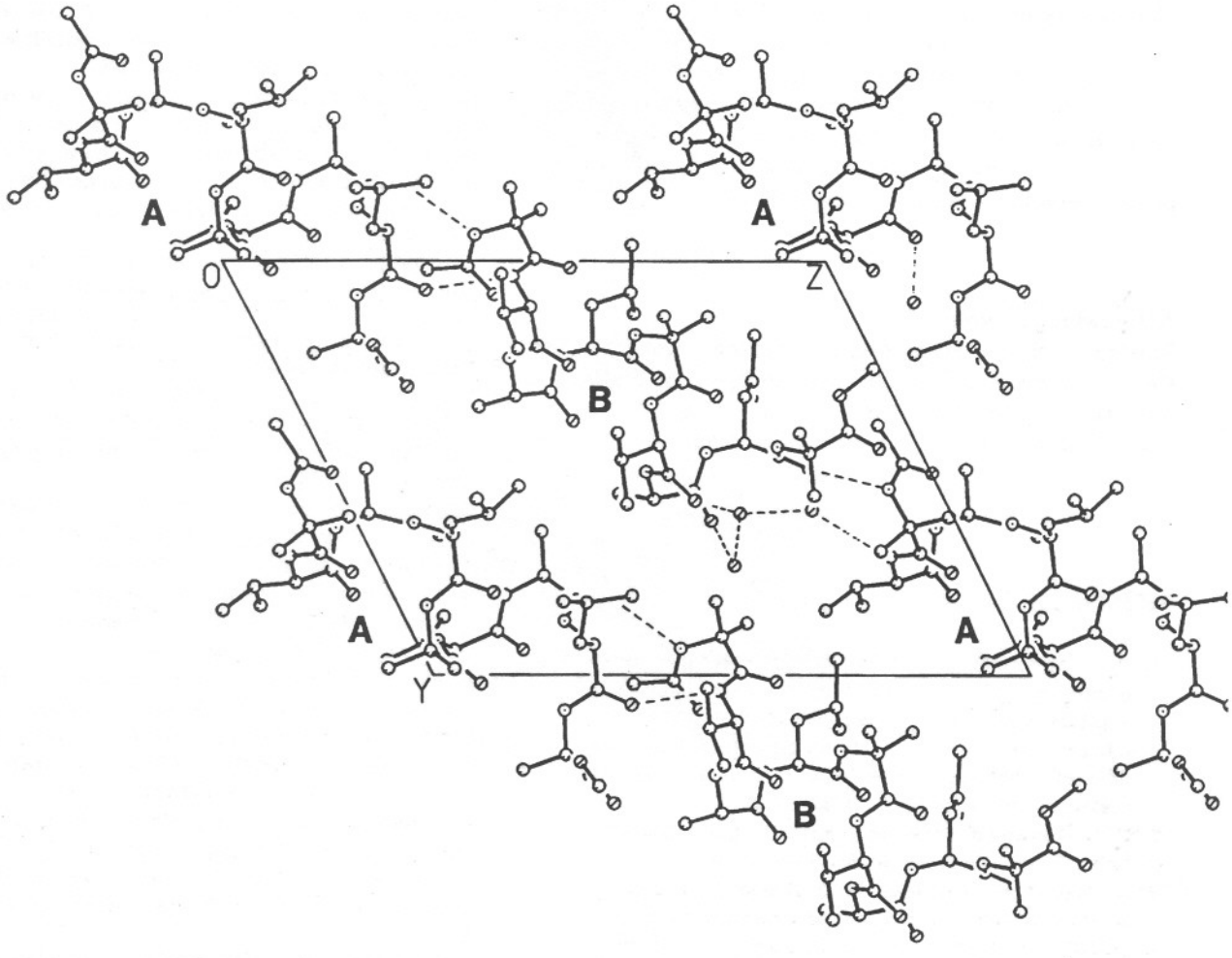

Figure 3 Packing diagram of molecules A and B of Ac-Aib-Val-Ala-Leu-Aib-Val-Ala-Leu-Aib-OMe. The view is down the *x*-axis. The helix axes of the continuous columns formed by head-to-tail hydrogen bonding are all parallel.

conformers A and B in the continuous column of helices formed by head-to-tail hydrogen bonding. The common arrangement that has been observed in other crystals is a repetition of the same molecule by simple translation in the direction of the helix axis or by a twofold screw action.

The similarity of the crystal state conformations of both the acetyl- and Boc-protected derivatives of the nonapeptide suggests that end group effects are minimal in determining stereochemistry and packing in these moderate-sized hydrophobic, helical peptides. Several general features emerge from these analyses of helical peptides in crystals: **(a)** helix orientation in crystals (parallel or antiparallel) cannot be readily rationalized; **(b)** when the asymmetric unit contains multiple molecules, the observed backbone conformations are generally similar, with only subtle variations of hydrogen bond patterns; **(c)** specific patterns of lateral association are not observed for side chains like Ala, Aib, Val and Leu, with space-filling considerations appearing to be dominant; **(d)** hydration is frequently observed, with water acting as a bridge between peptide molecules within a helical column. Water insertion into the helix backbone is also observed, albeit less frequently. The structure of the nonapeptide described in the present paper exemplifies many of these features.

Acknowledgements

This research was supported in part by a grant from the Department of Science and Technology, India and by the National Institute of Health Grant GM30902 and the Office of Naval Research.

REFERENCES

1. B. V. V. Prasad and P. Balaram (1984). The stereochemistry of α-aminoisobutyric acid containing peptides. *CRC Crit. Rev. Biochem. 16*, 307–347.
2. I. L. Karle and P. Balaram (1990). Structural characteristic of α-helical peptide molecules containing Aib residues. *Biochemistry 29*, 6747–6756.
3. C. Toniolo and E. Benedetti (1991). The polypeptide 3_{10}-helix. *Trends Biochem. Sci 6*, 350–353.
4. V. Pavone, E. Benedetti, B. Di Blasio, C. Pedone, A. Santini, A. Bavoso, C. Toniolo, M. Crisma and L. Sartore (1990). The longest regular polypeptide 3_{10}-helix at atomic resolution. *J. Mol. Biol 214*, 633–635.
5. J. D. Augspurger, V. A. Bindra, H. A. Scheraga and A. Kuki (1995). Helical stability of *de novo* designed α-aminoisobutyric acid-rich peptides at high temperatures. *Biochemistry 34*, 2566–2576.
6. I. L. Karle (1992). Folding, aggregation and molecular recognition in peptides. *Acta Cryst B48*, 341–356.
7. I. L. Karle, J. L. Flippen-Anderson, R. Gurunath and P. Balaram (1994). Facile transition between 3_{10}- and α-helix: structure of 8-, 9-, and 10-residue, peptides containing the -(Leu-Aib-Ala)$_2$-Phe-Aib fragment. *Protein Sci 3*, 1547–1555.
8. G. R. Marshall, E. E. Hodgkin, D. A. Langs, G. D. Smith, J. Zabrocki and M. T. Leplawy (1990). Factors governing helical preferences of peptides containing multiple α,α-dialkyl amino acids. *Proc. Natl. Acad. Sci. USA 87*, 487–491.
9. I. L. Karle, J. L. Flippen-Anderson, M. Sukumar and P. Balaram (1992). Helix packing in peptide crystals as models for proteins. A distorted leucine ladder in the structure of a leucine rich decapeptide. *Proteins: Struct., Function Genet 12*, 324–330.
10. I. L. Karle, J. L. Flippen-Anderson, M. Sukumar and P. Balaram (1992). Differences in hydration and association of helical Boc-Val-Ala-Leu-Aib-Val-Ala-Leu-(Val-Ala-Leu-Aib)$_2$-OMe.xH$_2$O in two crystalline polymorphs. *J. Med. Chem 35*, 3885–3889.
11. B. Di Blasio, V. Pavone, M. Saviano, A. Lombardi, F. Nastri, C. Pedone, E. Benedetti, M. Crisma, M. Anzolin and C. Toniolo (1992). Structural characterization of the β-bend spiral: crystallographic analysis of two long (L-Pro-Aib)$_n$ sequential peptides. *J. Am. Chem. Soc 114*, 6273–6278.
12. I. L. Karle, J. L. Flippen-Anderson, K. Uma and P. Balaram (1993). Peptide mimics for structural features in proteins. Crystal structures of three heptapeptide helices with a C-terminal 6 → 1 hydrogen bond. *Int. J. Peptide Protein Res 42*, 401–410.
13. I. L. Karle, J. L. Flippen-Anderson, K. Uma and P. Balaram (1993). Unfolding of an α-helix in crystals by solvation: Conformational fragility in a heptapeptide. *Biopolymers 33*, 827–837.
14. C. Toniolo, G. M. Bonora, A. Bavoso, E. Benedetti, B. Di Blasio, V. Pavone and C. Pedone (1985). Molecular structure of peptaibol antibiotics: solution conformation and crystal structure of the octapeptide corresponding to the 2–9 sequence of emerimicins III and IV. *J. Biomol. Struct. Dyn 3*, 585–598.
15. V. Pavone, E. Benedetti, B. Di Blasio, C. Pedone, A. Santini, A. Bavoso, C. Toniolo, M. Crisma and L. Sartore (1989). Critical main-chain length for conformational conversion from 3_{10}-helix to α-helix in polypeptides. *J. Biomol. Struct. Dyn 7*, 1321–1331.
16. I. L. Karle, J. L. Flippen-Anderson, K. Uma and P. Balaram (1988). Aggregation studies in crystals of apolar helical peptides: Boc-Aib-Val-Ala-Leu-Aib-Val-Ala-Leu-Aib-OMe. *Int. J. Peptide Protein Res 32*, 536–543.
17. K. Uma (1991). Modular design of synthetic protein mimics. Construction of helices. PhD Thesis, Indian

Institute of Science, Bangalore. Thesis Abstr. (1991) *J. Indian Inst. Sci 71*, 395–398.

18. E. Egert and G. M. Sheldrick (1985). Search for a fragment of known geometry by integrated Patterson and direct methods. *Acta Cryst A41*, 262–268.
19. J. Karle (1968). Partial structure information combined with the tangent formula for non-centrosymmetric crystals. *Acta Cryst B24*, 182–186.
20. G. M. Sheldrick (1992). SHELXTL PLUS, Release 4.2 for Siemens R3m/V Crystal Research System. Siemens Analytical X-ray instruments, Madison, Wisconsin, USA.
21. IUPAC-IUB Commission on Biochemical Nomenclature (1970). Abbreviations and symbols for the description of the conformation of polypeptide chains. *Biochemistry 9*, 3471–3479.